Molecular dialogue in the nitrogen-vixing root symbiosis Casuarina/Frankia : characterization of Frankia's symbiotic signal molecules

Marion Boisseaux

Master's thesis

Written by

Marion BOISSEAUX

Submitted for the degree of Engineer in Horticulture and Landscaping of Agrocampus-Ouest, Angers,

Major in Environmental Management of Ecosystems and Tropical Forests

Molecular dialogue in the nitrogen-fixing root symbiosis *Casuarina/Frankia*:

characterization of *Frankia*'s symbiotic signal molecules.

Publicly defended on 27 September 2018

AgroParisTech,

Montpellier

In front of the following committee:

Dr Claude PLASSARD	Examiner
Dr Valérie HOCHER	Internship supervisor
Dr Raphaël MANLAY	Academic tutor at AgroParisTech

ACKNOWLEDGMENTS

I am using this opportunity to express my deepest gratitude and special thanks to my three supervivors, Alyssa Carré-Mlouka, Valérie Hocher and Djamel Gully for their precious guidance which were extremely valuable for my study both theoretically and practically. I would also like to thank Hassen Gherbi and Sergio Svistoonoff for the interesting discussions.

The internship opportunity I had with the LSTM research team was a great chance for learning and professional development. I also want to thank Robin Duponnois for welcoming me in the LSTM research team. I am also grateful for having a chance to meet so many wonderful people and professionals who led me though this internship period. I am very grateful to Guillaume Cazals who took the time to explain mass spectrometry. I warmly thank my peers for their support and great work atmosphere. I would like to offer my special thanks to Perrine Ramberg who helped me daily in the laboratory.

Advice given by Raphaël Manlay has been a great help during my internship search and for his valuable advice.

I will strive to use gained skills and knowledge in the best possible way.

RÉSUMÉ

Les symbioses nodulaires fixatrices d'azote concernent les légumineuses et les plantes actinorhiziennes qui s'associent respectivement avec les bactéries diazotrophes du sol rhizobia et *Frankia*. Chez les légumineuses modèles, l'initiation de la symbiose nécessite un dialogue moléculaire entraînant chez les rhizobia la production de molécules signal appelées facteurs Nod. Chez les symbioses actinorhiziennes, la nature des signaux émis par la bactérie *Frankia* n'est pas connue mais semble différente de celle des facteurs Nod. L'objectif de ce stage est de caractériser et d'identifier le(s) molécule(s) signal de *Frankia*, impliquées lors de la symbiose entre l'arbre tropical *Casuarina glauca* et son microsymbionte *Frankia casuarinae*. Pour y parvenir, nous avons purifié des surnageants bactériens sur différentes surfaces chromatographiques. De plus, la stabilité des surnageants bactériens a été testée en réponse à des variations de pH et à l'action d'enzymes. Chaque analyse est validée par un biotest basé sur l'induction précoce de l'expression du gène symbiotique *CgNIN* dans les racines de jeunes plantules. Le(s) molécule(s) signal de *Frankia* ont une masse moléculaire comprise entre 0.5 et 3 kDa, sont hydrophile(s) et chitinase-résistante(s) avec un pI compris entre 1.8 et 7. Des analyses structurales ont mis en évidence la présence de motifs glycosilés.

Mots clefs: Symbiose actinorhizienne, *Casuarina glauca*, *Frankia*, molécule(s) signal, NIN Activator.

ABSTRACT

Nitrogen fixing root symbioses include both legumes and actinorhizal plants that are able to establish a symbiotic relationship with diazotrophs soil bacteria, called rhizobia and *Frankia* respectively. The most known legumes/rhizobia interaction is highly specific and depends on the plant recognition of symbiotic signaling molecules produced by rhizobia, called Nod Factors. In the case of actinorhizal symbioses, early bacterial symbiotic signaling molecules are still unknown, but findings suggest structural differences with rhizobial Nod Factors. Here, we aimed to characterize *Frankia casuarinae*'s signaling molecule(s) in the interaction with its actinorhizal host *Casuarina glauca*. We purified bacterial supernatant by using different chromatographic surfaces. We also investigated the stability of bacterial supernatants at different pH and their sensitivity to different enzymes. Purified fractions were then tested using a bioassay based on the expression of *CgNIN*, a symbiotic gene, induced at preinfection stages in seedlings' roots. Signal molecule(s) have a molecular weight between 0.5 and 3 kDa, are hydrophilic, resistant to a chitinase digestion, and active with a pI between 1.8 and 7. We obtained a significant amount of purified signal molecules to start structural analysis which indicated the presence of glycosylated molecules.

Key words: Actinorhizal symbiosis, *Casuarina glauca*, *Frankia*, signal molecule(s), NIN Activator.

TABLE OF CONTENTS

1. INTRODUCTION

1.1. SUSTAINABLE DEVELOPMENT AND SYMBIOTIC NITROGEN FIXATION

Nitrogen is abundant (78%) in the Earth's atmosphere in the form of dinitrogen (N_2) gas, yet most organisms are unable to metabolize N_2 because it is relatively inert. Fixed forms of nitrogen, such as ammonia (NH_3) or nitrate (NO_3^-) are continuously sequestered into sediments and also converted to N_2 through the combined processes of nitrification and denitrification, rendering them unavailable for plant metabolism. N_2 fixation occurs in three different ways: (i) through geochemical processes such as lightning, (ii) industrially through the Haber–Bosch process, and (iii) biologically through the action of the nitrogenase, enzyme found only in a select group of microorganisms (Hoffman *et al.*, 2014).

Conventional agriculture depends upon the Haber-Bosch process to produce the commercial fertilizer needed to grow most of the world's hybrid crops. But this approach comes with many environmental consequences, including the use of fossil fuels such as natural gas to produce this fertilizer. The Intergovernmental Panel on Climate Change (IPCC) also estimates that 1% of the nitrogen fertilizer is lost in the form of N_2O, equivalent to 300 million metric tons of CO_2 (Good, 2018). With growing environment-related concerns, there is renewed interest in biological nitrogen fixation as a way of limiting chemical fertilizers whose excessive use in past decades has contributed to greenhouse gas emissions and underground water pollution (Olivares, Bedmar, and Sanjuán, 2013; Santi, Bogusz, and Franche, 2013).

Only diazotroph bacteria can convert atmospheric nitrogen into ammonia. These organisms utilize the nitrogenase enzyme to catalyze the conversion of atmospheric nitrogen (N_2) to ammonia (NH_3). The reduction of atmospheric nitrogen is a complex process that requires a large input of energy to proceed (Postgate, 1982). Several plants have developed beneficial symbioses with diazotrophs in order to acquire atmospheric nitrogen. In a nitrogen-deficient soil, the diazotroph bacteria will convert atmospheric nitrogen into ammonia, which the plant can assimilate. In return, the plant will host the bacteria and provide carbon photosynthates. Among the nitrogen fixing symbioses, some of them lead to the formation of a new organ in the root area of the plant, called the "root nodule" (Pawlowski and Demchenko, 2012). Root nodule symbioses concerns two main groups of diazotrophs (Vessey, Pawlowski, and Bergman, 2005):

1. Rhizobia in association with legumes and one non-legume (*Parasponia*).
2. *Frankia* in association with actinorhizal plants.

Molecular phylogeny of plant groups that engage in root nodule symbioses shows that they all belong to a single lineage, the *Fabid* clade, and suggest a common ancestor with a predisposition for nodulation (Soltis *et al.*, 1995 ; Griesmann *et al.*, 2018) (Figure 1).

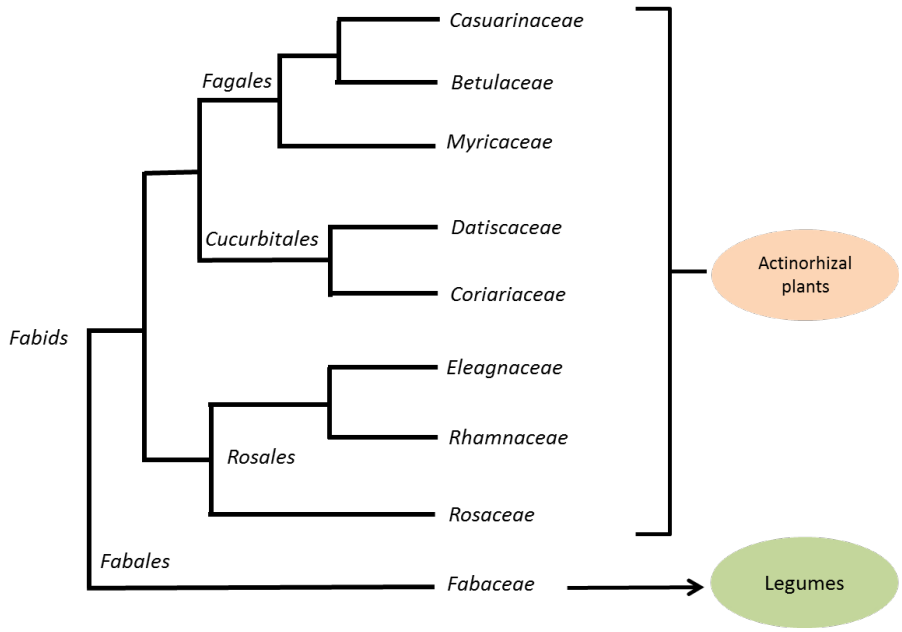

Figure 1: Phylogenic tree of the eight actinorhizal families and the one legume family that form root nodule symbioses, all belonging to the *Fabid* clade (Perrine-Walker *et al.*, 2011).

1.2. ACTINORHIZAL SYMBIOSES

1.2.1. HOSTS PLANTS IN THE ACTINORHIZAL SYMBIOSES

Rhizobial symbioses have received a lot of attention because several legumes are important crop species. Actinorhizal plants forming symbioses with *Frankia*, have been less studied and are still poorly understood (Dawson, 2008), even though they play an important ecological role and their contribution to nitrogen soil fertility is of great environmental value in many areas (Zhong *et al.*, 2013). When compared on a fresh weight, nitrogen fixation rates of actinorhizal plants are of the same order of magnitude as those observed in the legume-rhizobia symbiosis. In temperate climates, nitrogen-fixation activity in actinorhizal plants could be similar to the rate of 300 $kg.ha^{-1}.year^{-1}$ measured in legumes (Santi, Bogusz, and Franche, 2013). Actinorhizal symbioses include approximately 280 plant species that are part of eight angiosperm families from three orders: the *Fagales* (*Betulaceae*, *Casuarinaceae* and *Myricaceae*), the *Rosales* (*Rosaceae*, *Eleagnaceae* and *Rhamnaceae*) and the *Cucurbitales* (*Datiscaceae* and *Coriariaceae*) (Figure 1).

Among actinorhizal plants, *Casuarina* species are widely planted since it has been proved to grow best under tropical and mediterranean climates and can adapt to difficult sites (Simonet *et al.*, 1999). *Casuarina* species are both economically and ecologically important as they provide a wide range of goods and services. Casuarinas are a major source of fuelwood and charcoal and is also used for construction. Casuarinas have been used in agroforestry, for example mixed with pineapples in China, planted as windbreaks around cultivated fields to stabilize drifting sand and have also been used in general soil rehabilitation programs such as former mining sites (Figure 2) (Zhong *et al.*, 2013).

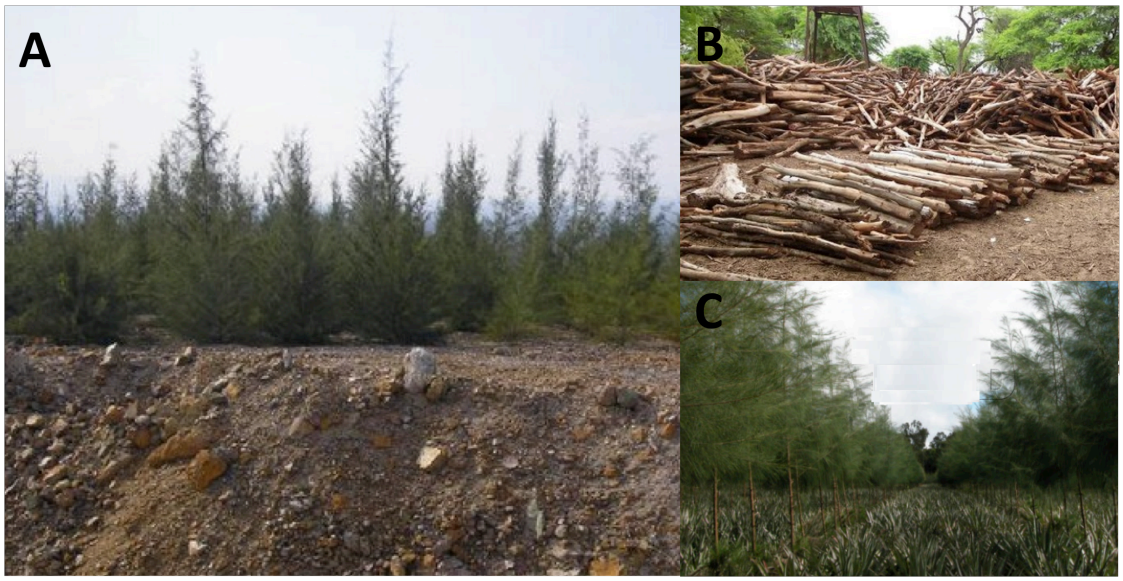

Figure 2: Uses of *Casuarinaceae*. **A:** *Casuarina* plantation in Niayes region for fixation of dunes, Senegal. **B:** *Casuarina* wood used as firewood. **C:** Agroforestry mixing pineapple and *Casuarinaceae* in China. (Diagne *et al.*, 2013)

Casuarina glauca Sieb. Ex Spreng., commonly known as swamp-she oak, belongs to the family *Casuarinaceae* in the order *Fagales* (Figure 3). This medium-sized deciduous tree (8–20 m high) is native to the east coast of Australia (National Research Council 1984). The leaves are reduced to lanceolate scales about 1 mm long, thereby reducing evapotranspiration and contributing to the adaptation of *Casuarina* trees to arid and semi-arid climates. In addition, *Casuarina* trees are able to develop a symbiotic association with endomycorrhizae, which increases nutrient uptake such as phosphorus (Zhong *et al.*, 2013).

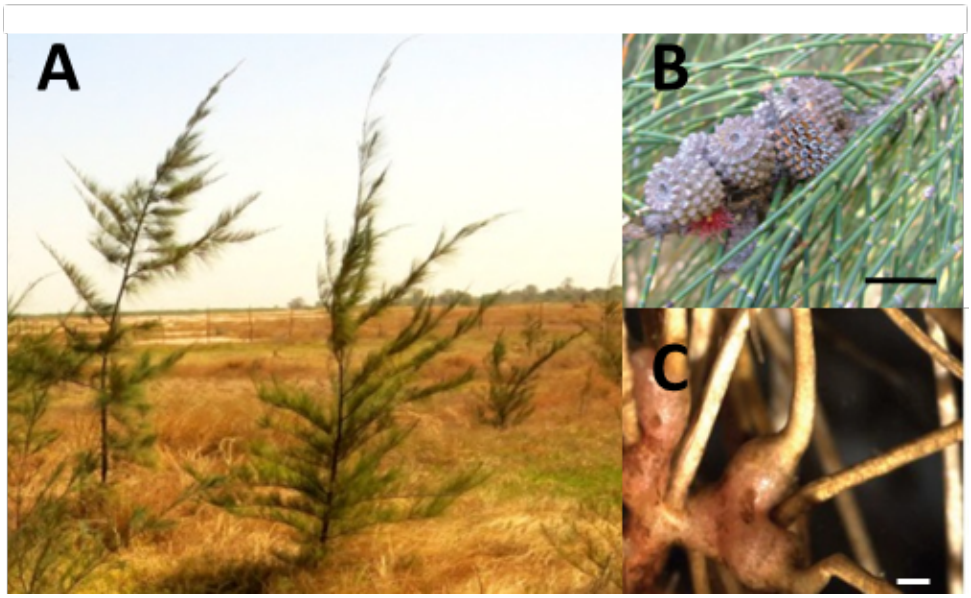

Figure 3: *Casuarina glauca* tree morphological traits. **A:** *Casuarina glauca* trees. **B:** *Casuarina glauca* branches with fruits, bar = 1 cm. **C:** Actinorhizal root nodule, bar = 1 mm. (Svistoonoff *et al.*, 2013)

1.2.2. BACTERIAL PARTNER: *FRANKIA*

Frankia is a Gram-positive nitrogen-fixing actinobacterium that forms a symbiotic association with actinorhizal plants. The species belongs to the order *Frankiales* and the family *Frankiaceae*. It is a filamentous bacterium (Normand *et al.*, 1996) found in root nodules or in soil (Chaia, Wall, and Huss-Danell, 2010). This bacterium is characterized by a high G + C% genome content (70%) and a slow growth rate (Benson and Silvester, 1993). In liquid culture and depending on the condition of culture, *Frankia* forms hyphae and multilocular sporangia (Figure 4). Other morphological structures are vesicles, which are the site of nitrogenous activity and are generally formed when nitrogen is very limited in the medium (Zhang and Benson, 1992). Callaham isolated in 1978 the first effective strain of *Frankia* (Rouvier *et al.*, 1996), and since then many strains have been isolated. Due to the difficulty involved in developing tools for genetic analysis in *Frankia*, today there is no way to knock down or over-express targeted genes in any *Frankia* strain. Gene transfer can be transiently achieved by electroporation, but no stable transformants have been obtained (Kucho *et al.*, 2009).

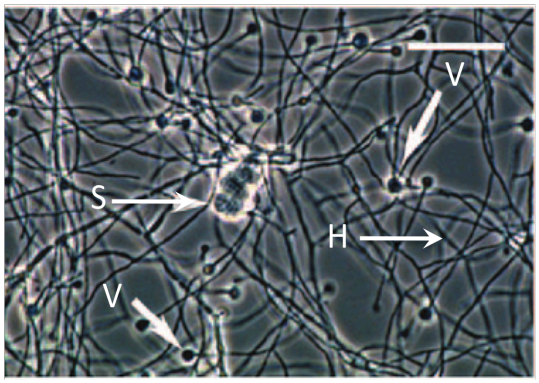

Figure 4: Morphology of *Frankia* in pure liquid culture. Arrows point to vesicles (V), hyphae (H), sporangia (S), bar, = 20 μm. (Valdés *et al.*, 2005)

Genomic studies have been undertaken to characterize *Frankia* (Normand *et al.*, 2007). In recent years, 36 genomes of *Frankia* have been sequenced, including the genome of *Frankia casuarinae*, which can nodulate *C. glauca* (Normand *et al.*, 2007; Rawnsley and Tisa, 2007) The average size of *Frankia*'s genome is around 8 Mbp and genome of *Frankia casuarinae* is one of the smallest, with 5.43 Mbp (Tisa *et al.*, 2016).

1.2.3. ROOT NODULE FORMATION

Root nodule formation in actinorhizal plants occurs in several stages that require a series of interactions between the bacteria and host root cells (Obertello *et al.*, 2003) (**Figure 5**). The bacteria must recognize its host plant, attach to the surface, and penetrate the root. *Frankia* can infect host plants by two distinct routes: (1) intercellular penetration of root epidermis cells and cortex cells, which is the case of the Patagonian shrub Discaria, and (2) intracellular penetration of a plant epidermal cell at a bend in a deformed root hair (Berry, McIntyre, and McCully, 1986) which is the case in the *Casuarina-Frankia* symbiosis. Some *Frankia* strains are capable of infecting host plants by both routes, but the method of entry is dictated by the host plant (Miller and Baker, 1986).

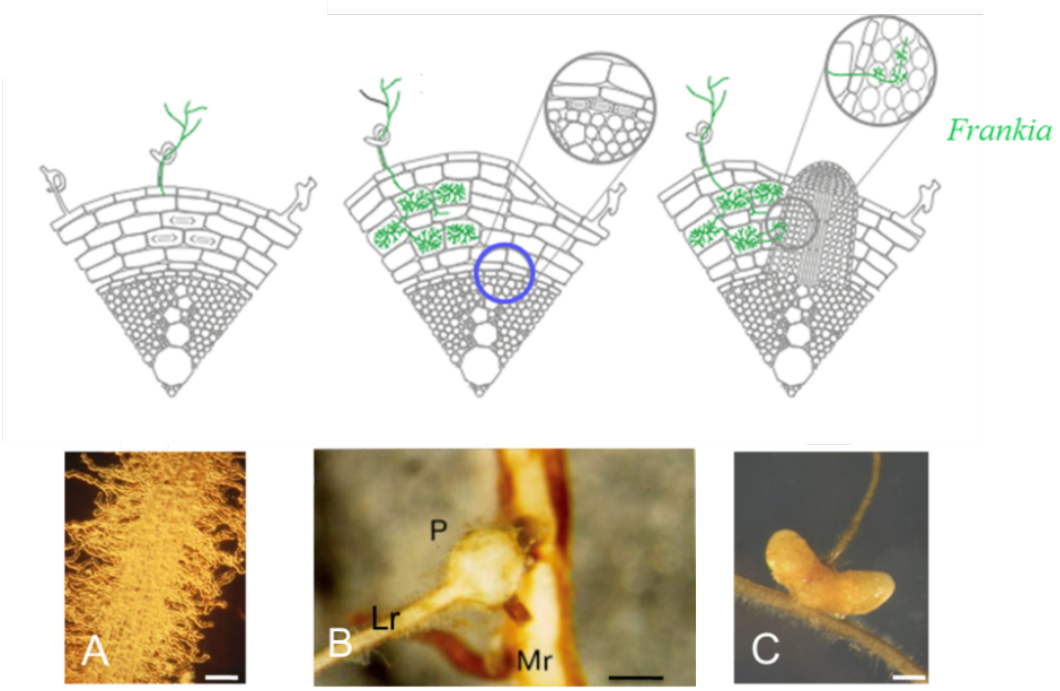

Figure 5: Intracellular infection process and root nodule development in the *Casuarina glauca-Frankia casuarinae* symbiosis.
A: After molecular signal exchange between the plant and the bacteria, *Frankia* penetrates a deformed root hair and induces cortical cellular divisions. Bar = 100 µm. **B:** Cortical dividing cells are infected by *Frankia*'s hyphae generating the prenodule (P). Lateral root (Lr), Main root (Mr). Bar = 500 µm. Cell divisions are induced in the pericycle in front of a xylem pole (blue circle), generating a nodular primordium. **C:** The nodule cortex becomes infected intracellularly by *Frankia*'s hyphae coming from the prenodule. The mature nodule shows a similar structure to a modified lateral root. Bar = 1 mm. (Adapted from Péret *et al.*, 2007)

In the case of intracellular penetration, an infection thread is established that is composed of a mass of bacteria encapsulated by a polysaccharide matrix produced by the host (VandenBosch and Torrey, 1985). As the infection progresses, limited cell divisions occur close to the infection site generating a prenodule (Baker and Mullin, 1992). Some prenodule cells become infected by *Frankia* and differentiate to fix nitrogen. At the same time, cell divisions are induced in the pericycle in front of a xylem pole. These divisions give rise to a nodule lobe primordium. As the nodule lobe primordium grows, the nodule cortex becomes infected intracellularly by *Frankia* hyphae coming from the prenodule. The nodule is the site of nitrogen fixation in the plant. The shape and internal structure of the nodule is plant-dependent (Baker and Mullin, 1992). In the field, actinorhizal nodules can have variable forms and colors (Bargali, 2011). The nodules can reach up to 10 cm in diameter (Zhong *et al.*, 2013).

1.3. SYMBIOTIC SIGNALIZATION IN ROOT NODULE SYMBIOSES

1.3.1. LEGUME – RHIZOBIA SYMBIOSES

Symbiotic associations are achieved through chemical communication between the microorganism and the host plant root (Oldroyd, 2013). In legumes, recognition between the plant and the bacteria is mediated through flavonoids released by the plant root. In return, rhizobia express canonical *nodABC* genes responsible for the synthesis of

nodulation factors (Nod factors) that are recognized by the plant to activate the symbiosis signaling pathway (Lerouge *et al.*, 1990). Nod factors are lipo-chito-oligosaccharide compounds, and for each rhizobial species the length of the chitooligosaccharide backbone and the type of substitutions at both ends of the molecule differs (Dénarié, Debellé, and Promé, 1996). Nod factors are thus symbiosis-specific and sufficient to activate nodule organogenesis and induce cellular changes associated with the initiation of bacterial infection (Oldroyd *et al.*, 2011). The perception of bacterial Nod factors by model legume plants induces a range of responses including ion fluxes, rhythmic Ca^{2+} oscillations (spiking) and changes in gene expression patterns. Nod factors also trigger root hair deformation, which has been used as a bioassay to identify the chemical nature of Nod factors (Lerouge *et al.*, 1990; Oldroyd, 2013). Using gene silencing methods and mutant screenings, genes such as *SYMRK* (SYMbiosis Receptor Kinase), *CCaMK* (Calcium & Calmodulin-dependent Kinase) or *NIN* (Nodule Inception) were shown to be essential to the nodulation process. The *NIN* gene has been extensively studied for its roles during early and late stages of nodulation (Guillotin, Couzigou, and Combier, 2016). First identified in *Lotus japonicus*, this gene is specific to nodulation (Oldroyd, 2013). The inactivation of the mutant *ljnin* (*NIN* gene in *Lotus japonicus*) failed to form nodules following inoculation. *NIN* is a key transcriptional factor in nodule development. *NIN* also acts as a negative regulator, inhibiting additional Nod factors responses after the initial activation of this signaling pathway to regulate the number of nodules (Yoro *et al.*, 2014; Soyano *et al.*, 2014).

1.3.2. ACTINORHIZAL SYMBIOSES

Compared to legumes, actinorhizal symbioses have been less studied and little is known about their symbiotic signaling pathway. Transcriptomics studies developed in *C. glauca* and *Datisca glomerata* revealed that some components of the Nod factor signaling pathway were also present in actinorhizal plants (Hocher *et al.*, 2006; Hocher *et al.*, 2011; Demina *et al.*, 2013). At least both the kinase receptor SYMRK and the Calcium & Calmodulin-dependent protein kinase CCaMK are present and essential to actinorhizal symbiosis (Gherbi *et al.*, 2008; Markmann, Giczey, and Parniske, 2008; Svistoonoff *et al.*, 2013). These findings reinforce the hypothesis of a common pathway for root endosymbioses (Svistoonoff, Hocher, and Gherbi, 2014). *CgNIN* was identified as the ortholog of the legume *NIN* gene. In *C. glauca*, *CgNIN* is expressed in the early stages of nodulation and takes part in the specific signaling pathway of actinorhizal and legume plants (Clavijo *et al.*, 2015). Calcium spiking reaction, another common element to the signaling pathway of nitrogen fixing root symbioses was recently demonstrated in *Alnus glutinosa* and *C. glauca* in response to *Frankia* (Granqvist *et al.*, 2015; Chabaud *et al.*, 2016).

On the bacterial side, little is known about *Frankia* symbiotic signaling molecules. Using *Alnus glutinosa* root hair deformation as a bioassay, *Frankia alni* was shown to secrete factors, which share some properties with the Nod factors (activity at very low concentrations, thermostability) (Cérémonie, Debellé, and Fernandez, 1999). However, this factor called Root Hair Deforming Factor (RHDF) is not yet characterized. Moreover, canonical *nodABC* genes were not found in most of the sequenced genomes of 36 *Frankia* strains including *Frankia casuarinae* (Tisa *et al.*, 2016). Only a few low-similarity homologs of *nodB* and *nodC* were detected in the *Frankia alni* genome, scattered throughout the genome and located far away from other symbiosis-related genes (Normand *et al.*, 2007), suggesting thus that different genes and molecules might be involved in the actinorhizal signaling. Recently, canonical *nodABC* genes have been found in the genomes of two uncultured *Frankia* strains (Persson *et al.*, 2015 ; Nguyen *et al.*,

2016) and in one isolated strain (Ktari *et al.*, 2017). However, their involvement in symbiotic signaling is still unknown.

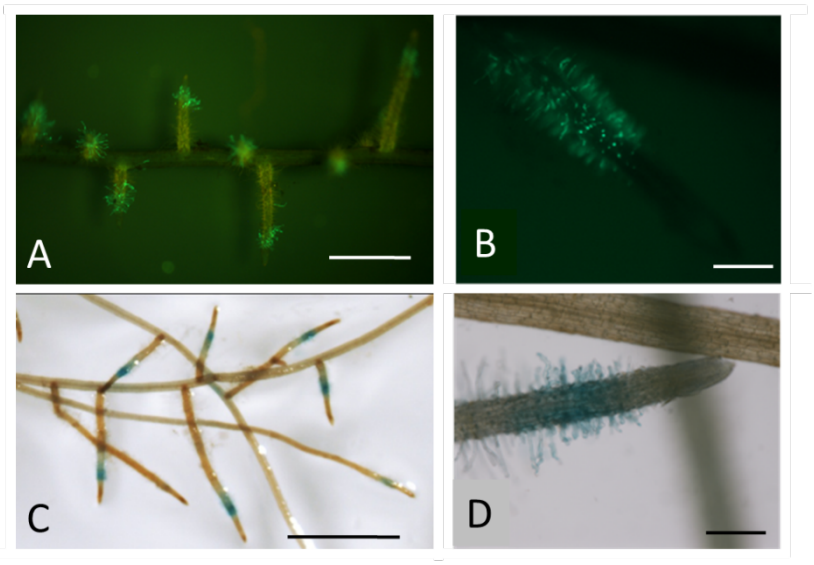

Figure 6: Activation of *ProCgNIN* in *C. glauca* root hairs after 16 hours incubation with *F. casuarinae* supernatant.
A: GFP fluorescence observation in lateral roots of Pro*CgNIN:GFP* plant, bar = 2 mm. **B**: GFP fluorescence observation in root hairs of Pro*CgNIN:GFP* plant, bar = 500 µm. **C:** GUS coloration observation in lateral roots of *ProCgNIN:GUS* plant, bar = 2 mm. **D**: GUS coloration observation in root hairs of *ProCgNIN:GUS* plant, bar = 500 µm. (Photo credits from S. Svistoonoff)

To better understand the infection process in the actinorhizal symbiosis, a specific bioassay was developed using plant genes that are specifically expressed in response to the interaction with compatible *Frankia*. We focused on the symbiosis *C. glauca* / *F. casuarinae* as transgenic *C. glauca* plants with the construction Pro*CgNIN:GUS* and Pro*CgNIN:GFP* were already generated (Clavijo *et al.*, 2015). GUS and GFP are both reporter genes attached downstream to the promoter of *CgNIN*. Characterization of *CgNIN* expression revealed that after contact with either the bacteria *F. casuarinae* or its cell-free supernatant (FcS), the *CgNIN* promoter was activated from 12 hours to 48 hours (Clavijo *et al.*, 2015). A characteristic fluorescence or GUS signal can then be observed in the root hairs of Pro*CgNIN:GUS* and Pro*CgNIN:GFP* plants (Figure 6).

This bioassay is thus a good tool for developing a bioguided purification of *Frankia casuarinae* symbiotic signal molecules and its use led to the characterization of a *Frankia casuarinae* symbiotic factor called NINA (*NIN*-Activator) (Chabaud *et al.*, 2016). NINA has been partially characterized and previous results have shown that it is a small size (1-3 kDa), thermostable molecule. While rhizobial Nod factors are amphiphilic chitin-based molecules, NINA is hydrophilic and resistant to chitinase, thus suggesting a different chemical nature for *Frankia* symbiotic factor(s) (Chabaud *et al.*, 2016). Although several physical and chemical properties for the NINA factor have been described, its exact chemical nature has not yet been determined (Cissoko *et al.*, 2018).

1.4. OBJECTIVES OF THE RESEARCH TEAM AND INTERNSHIP PROJECT

The overall objective of the SYAT (Symbioses of Tropical Actinorhizal Plants) team is the elucidation of the early signaling events in the symbiosis between actinorhizal plants and their bacterial partner. One of the current goals is to identify and characterize NINA, the symbiotic signal molecule(s) of *Frankia* in response to *F. casuarinae* supernatant (FcS). This project is developed in collaboration with the laboratory team of Professor Louis Tisa (University of New Hampshire, USA). This project is funded by the United States Department of Agriculture (USDA).

The focus question of my internship is: "What are *Frankia's* early symbiotic signal molecules in the molecular dialogue in the nitrogen-fixing root symbiosis *Casuarina glauca / Frankia casuarinae?*

My objectives are to continue the characterization of *Frankia*'s early signal molecules using a variety of biochemical methods. My first goal was to optimize a method for NINA's purification. To characterize the chemical nature of NINA, we tested its sensitivity to different enzymes and to different pH. The results of these experiments were then used for the development of a purification protocol based on the physical and chemical properties of NINA. We obtained a significant amount of semi-purified NINA which was used for preliminary structural analysis using mass spectrometry.

2. MATERIALS AND METHODS

2.1. BIOLOGICAL MATERIAL

2.1.1. PLANT MATERIAL

Transgenic *C. glauca* plants containing a Pro*CgNIN:GFP* or a Pro*CgNIN:GUS* construct described previously (Clavijo *et al.*, 2015) were grown in hydroponics in pots containing a modified Broughton and Dilworth medium supplemented with 1 mM KNO_3 (BD+N) and vegetatively propagated by cuttings as described previously (Zhong *et al.*, 2009). Plantlets were placed in a growth chamber kept at 26°C ± 1°C, under neon lighting at 150 $\mu E.m^{-2}.s^{-1}$, and a photoperiod of 16 h. After three weeks, rooted transgenic *C. glauca* plantlets were transferred to a hydroponic system consisting of plastic pots filled with 0.55 L of BD+N medium.

2.1.2. BACTERIAL MATERIAL

Frankia casuarinae (ex-strain CcI3) (Zhang, Lopez, and Torrey, 1984; Nouioui *et al.*, 2016) was used to produce supernatants (FcS). *Frankia* cultures were grown in a modified basic proprionate BAP medium without phosphatidylcholine as described previsously (Svistoonoff *et al.*, 2010). *F. casuarinae* cultures were induced with root exudates from *C. glauca* for 5 days according to Clavijo *et al.* (2015). *Frankia* cultures were then centrifuged at 3000 *g* for 5 min and the supernatants were filtered through a 0.2 µm filter, concentrated 50 fold using an R-210/215 evaporator (BUCHI Labortechnik AG, Switzerland), conditioned in 50 mL sterile tubes and stored at room temperature for further biochemical experiments (Cissoko *et al.*, 2018).

2.2. PLANT BIOASSAY DESIGN

The activation of Pro*CgNIN* in response to tested solutions was evaluated using transgenic Pro*CgNIN:GUS* and Pro*CgNIN:GFP* plants previously grown in hydroponics deprived of nitrogen for one week (Clavijo *et al.*, 2015; Chabaud *et al.*, 2016). For positive control, plant roots were incubated 24 h with a 1:100 dilution of FcS and for negative control, 1:100 dilution of BAP medium was used (Chabaud *et al.*, 2016; Cissoko *et al.*, 2018). For each test performed in our study, transgenic plants were incubated for 24 h with a final concentration of the tested solution equivalent to a 1:100 dilution of FcS to be comparable. For each treatment, there were four replicates since a treated pot contained four transgenic plants (one Pro*CgNIN:GUS* and three Pro*CgNIN:GFP*).

Plant GFP fluorescence was monitored in the short lateral root hairs using an AZ100 macroscope (Nikon) equipped with a 5X objective, a GFP filter (Excitation filter 470 nm ± 40 nm; Barrier filter 535 nm ± 50 nm; Nikon) and a digital camera Sight D5 RI1 (Nikon). Fluorescence level was evaluated manually, using the following arbitrary scale (Cissoko *et al.*, 2018): 0: no detectable fluorescence; 1: weak fluorescence; 2: intermediate fluorescence; and 3: strong fluorescence (Figure 7). To limit bias, all observations were performed by the same person. Within one experiment, positive control was observed first and considered the highest fluorescence level (level 3). For the treatments, fluorescence levels were estimated in comparison to the positive control. For each fluorescence level, the number of fluorescing plants was recorded and converted

into a percentage. For the pre-purification experiments, the median of the fluorescence level observed per treatment was calculated.

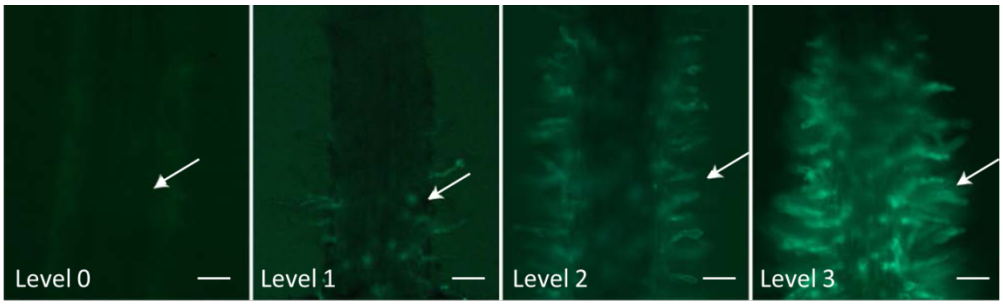

Figure 7: Scale of GFP fluorescence in root hairs of Pro*CgNIN:GFP C. glauca* plants. Level **0:** no detectable fluorescence; level **1:** weak fluorescence; level **2:** intermediate fluorescence; and level **3:** strong fluorescence. Arrows indicate root hairs, bars = 100 µm (Cissoko *et al.*, 2018).

For GUS revelation, samples of short lateral root hair were incubated for 24 h at 37 °C with a solution of 1 mM 5-bromo-4-chloro-3-indolyl glucuronide, 50 mM $NaPO_4$ pH 7, 1 mM Na_2-EDTA, , 0.5% Triton X100) (X-Gluc solution). Short lateral root hairs were then incubated for 24 h at 4°C with a 50% ethanol – 50% acetic acid solution and then kept in 70% ethanol at 4°C. Short lateral root hairs wet-mounts were observed between slide and slip using AZ100 macroscope (Nikon) under white light with a 5X objective. GUS plant results either showed a blue coloration or no coloration, and were used to confirm GFP plant results.

2.3. BIOCHEMICAL METHODS

Frankia casuarinae supernatants 50X were centrifuged at 7000 *g* during 10 min before dialysis. Supernatants were dialyzed for 12 h at 4°C against ultrapure water using 100-500 Da cutoff membrane (Float-A-Lyzer G2 dialysis devices, Spectrum Laboratories, USA). After dialysis, supernatant concentration was 30 fold (FcS 30X) and all experiments were done using FcS 30X as starting material.

2.3.1. TEST OF NINA SENSITIVITY TO pH BUFFERS

MES buffers (2-morpholin-4-yl-ethanesulfonic acid) (1 M) were prepared at pH 5, 6 and 7. TRIZMA buffers (2-amino-2-hydroxymethyl-propane-1,3-diol) (1 M) were prepared at pH 7 and 8. HEPES buffers (2-4-(2-hydroxyethyl)piperazin-1-yl-ethanesulfonic acid) (1 M) were prepared at pH 7 and 8. For all buffers, pH was adjusted using NaOH (1 M). FcS 30X was incubated with each buffer for 24 h at room temperature, before being tested using the plant bioassay.

2.3.2. TEST OF NINA SENSITIVITY TO ENZYMES

Proteinase K (V302B), Trypsine (T1426), Endoproteinase Glu-C (P2922), Asp-N (P3303) and Chitinase (C8241) from Sigma-Aldrich were used to prepare stock solutions of each enzyme at 10 $mg.mL^{-1}$. FcS 30X was digested at 37°C for at least 4 hours using a final enzyme concentration of 40 $\mu g.mL^{-1}$. Several controls were performed. For negative control, *F. casuarinae* medium culture (BAP) was digested in similar conditions. Effect of enzyme buffers alone was tested on FcS 30X: TRIS-HCl buffer pH 8 (1 M) and phosphate buffer pH 7.5 (KH_2PO_4 0.1 M, Na_2HPO_4 0.1 M). Phenylmethylsulfonyl

fluoride (PMSF) was used as enzyme inhibitor. Last, FcS 30X and BAP were incubated with buffers, either with enzyme at 37°C for at least 4 hours or without. Each digestion or control was tested using the plant bioassay.

2.3.3. SOLID PHASE EXTRACTION

Purification of NINA was performed using solid phase extraction (SPE) columns. One C18 (WATERS Sep-Pak ® cartridge) and four different types of ion exchange columns were tested. W-AX and W-CX respectively weak anion and weak cation exchange (Phenomenex 500 mg 3 mL) were first tried. Hybrid columns that combine ion exchange and polarity interactions were also tested to purify NINA: Strata X-AW (weak anion exchange) and Strata X-CW (weak cation exchange) (Phenomenex 500 mg 3 mL). The Phenomenex protocol (Phenomenex, 2017) was first applied and further modified in order to optimize NINA purification efficiency. All tested conditions are listed in Table 1. All loading, wash and elution fractions obtained were tested for Pro*CgNIN* activation using our plant bioassay. Fractions containing NINA were then concentrated 6000 fold using a centrifugal vacuum concentrator (Labconco acid-resistant centrivap concentrator). Unless otherwise specified, Strata X-CW elution fractions were then resuspended in 200 µL of ultra-pure water for further analysis.

Table 1: Phenomenex recommended protocol and summary of tested conditions to optimize the NINA purification protocol.

	Phenomenex protocol		Tested conditions	
Steps	**Solvent**	**Volume (mL)**	**Solvent**	**Volume (mL)**
Conditioning	1. Methanol 100% 2. Ultra-pure water pH 7	10 10	1. Methanol 100% 2. HEPES 20 mM pH 7	10 10
Sample loading	FcS 30X+ pH 7	10	FcS 30X + HEPES 20 mM pH 7; FcS 30X + MES 20 mM pH 7; FcS 30X + MES 20 mM pH 6; FcS 30X + MES 20 mM pH 5	10
Wash	1. Ammonium acetate 25 mM pH 7 or Ultra-pure water pH 7 2. Methanol 100%	10 10	1. Ammonium acetate 25 mM pH 7 2. Methanol 10%; Methanol 20%; Methanol 30%; Methanol 50%; Methanol 100%.	20 20
Elution	Methanol 95% / ammonium hydroxyde 5 % or Methanol 95% / formic Acid 5%	10 10	Methanol 95% / ammonium hydroxyde 5% Methanol 95% / formic Acid 5%	10 10

2.3.4. HIGH PRESSURE LIQUID CHROMATOGRAPHY

High pressure liquid chromatography (HPLC Waters Alliance 2690) was performed on previously obtained semi-purified samples with two columns, Reverse Phase Luna C18(2) (RP-C18) and Reverse Phase Luna Omega Polar C18 (RP-Polar C18) from Phenomenex. For each run, injection volume was 50 µL. Mobile phase consisted of ultra-pure water (solvent A) and methanol (solvent B) containing either 0.1% TFA or 0.1% ammonium hydroxide as additives. Gradient performed was 100% solvent A for 10 min; 0%-100% solvent B for 10 min; 100% solvent B for 5 min with a time out for 2 min. Flow rate was 1 mL.min^{-1} and detection was monitored at λ = 254 nm. Temperature

was controlled at 25°C. Every minute, 1 mL was manually collected and fractions were tested for their NINA activity using our plant bioassay.

2.3.5. MASS SPECTROMETRY

All experiments were performed at the Technological Platform Laboratory of Physics, Montpellier. Tandem quadrupole time-of-flight mass spectrometry (Q-TOF MS) and liquid chromatography paired with mass spectrometry (Q-TOF LC MS/MS) were performed using Synapt G2-S (Waters). For each run in LC MS/MS, injection volume was 1 µL. Mobile phase consisted of ultra-pure water (solvent C) and methanol (solvent D). Gradient performed was gradient elution for 2 min from 0% to 10% of solvent D; gradient elution for 3 min from 10% to 100% of solvent D; 100% solvent D for 1 min; 100% solvent C for 3 min. Flow rate was 0.5 $mL.min^{-1}$. Electrospray ionization (ESI) was the source used for sample analysis in both positive and negative ionization modes. The electric field used for the ion trap was 15 V to 60 V. MassLynx was the software used for spectra analysis.

2.3.6. STATISTICAL ANALYSES

All raw data are given in appendices. Statistical analyses were done on GFP fluorescence raw data using the basic functions of R (R Team, 2013). A Shapiro-Wilk normality test was performed followed by a non-parametric Kruskal-Wallis multiple comparison test and a pairwise Wilcoxon test. Statistical significance was recorded at *p-value<0.05.

3. RESULTS

3.1. CHEMICAL CHARACTERIZATION OF NINA

3.1.1. EFFECT OF pH ON Pro*CgNIN* ACTIVATION

To guide us in drafting a NINA's purification process, we first tested the activation of Pro*CgNIN* by *F. casuarinae* supernatant incubated at different pH using several buffers. Plant fluorescence was recorded (Appendix 1) and results are summarized in Figure 8. For negative control, buffers were tested on plants and did not induce fluorescence (data not shown).

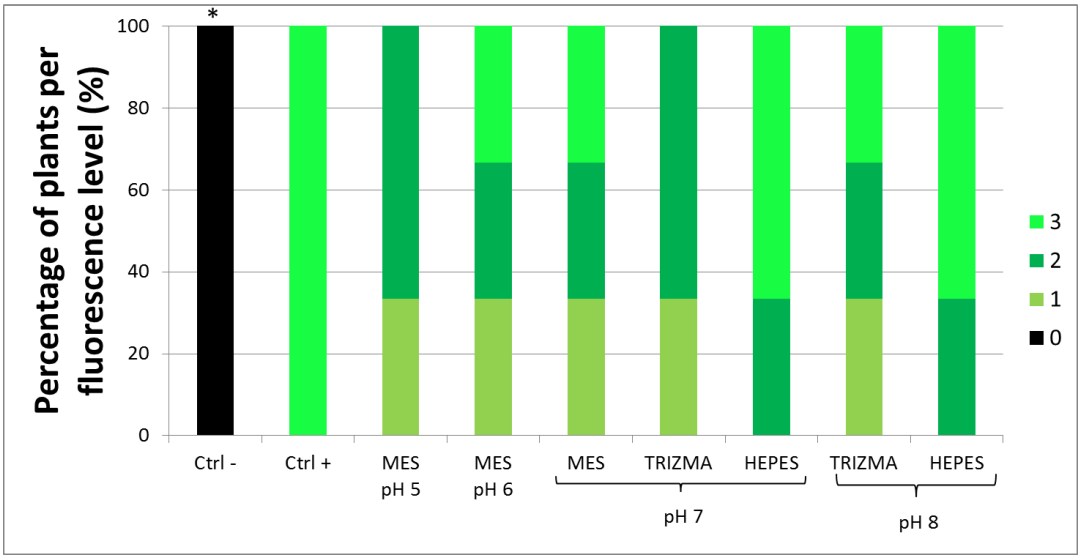

Figure 8: Effect of different pH using different buffers on the expression of Pro*CgNIN*. BAP was used for negative control (Ctrl-); *F. casuarinae* supernatant was used for positive control (Ctrl+). The different buffers and pH used to perform the experiment are written underneath the bar graph. Number of plants per fluorescence level scaled 0, 1, 2, 3 was counted and converted into percentages (§2.2). Statistical significance to the positive control was recorded at *p-value<0.05, n=3. Raw data are found in Appendix 1.

In our experiment, no significant differences were found between the different pH solutions tested (Figure 8). Only the negative control (Ctrl-) was significantly different from the positive control (Ctrl+). However, the incubation of FcS with different pH solutions seems to decrease the fluorescence in comparison to the positive control. To improve the robustness of our findings, more replicates should be performed.

For MES buffer at pH 5, fluorescence was lower than the positive control. For MES buffer at pH 6, plants observed showed a heterogeneous fluorescence response. For pH 7 and pH 8, fluorescence response was heterogeneous according to the buffer used. HEPES buffer showed the best fluorescence response, thus the best Pro*CgNIN* activation. GUS results confirmed GFP fluorescence results (Appendix 1).

When working in the pH range 5 to 7, we chose the MES buffer. For all the other experiments at pH 7, we chose HEPES buffer because results show a better *CgNIN* activation with HEPES than with MES or TRIZMA buffer.

3.1.2. EFFECT OF ENZYME DIGESTIONS ON Pro*CgNIN* ACTIVATION

To investigate NINA's chemical structure, we tested different enzymes on *F. casuarinae* supernatant and recorded the enzyme effect on Pro*CgNIN* activation. Three serine proteases with broad specificity, one chitinase and one metalloproteinase were tested, with or without the protease inhibitor PMSF (§2.3.2). Plant fluorescence was recorded (Appendix 2) and results were summarized in Figure 9. For negative control, enzymatic buffers alone with FcS were also tested on plants and did not induce fluorescence (Appendix 3).

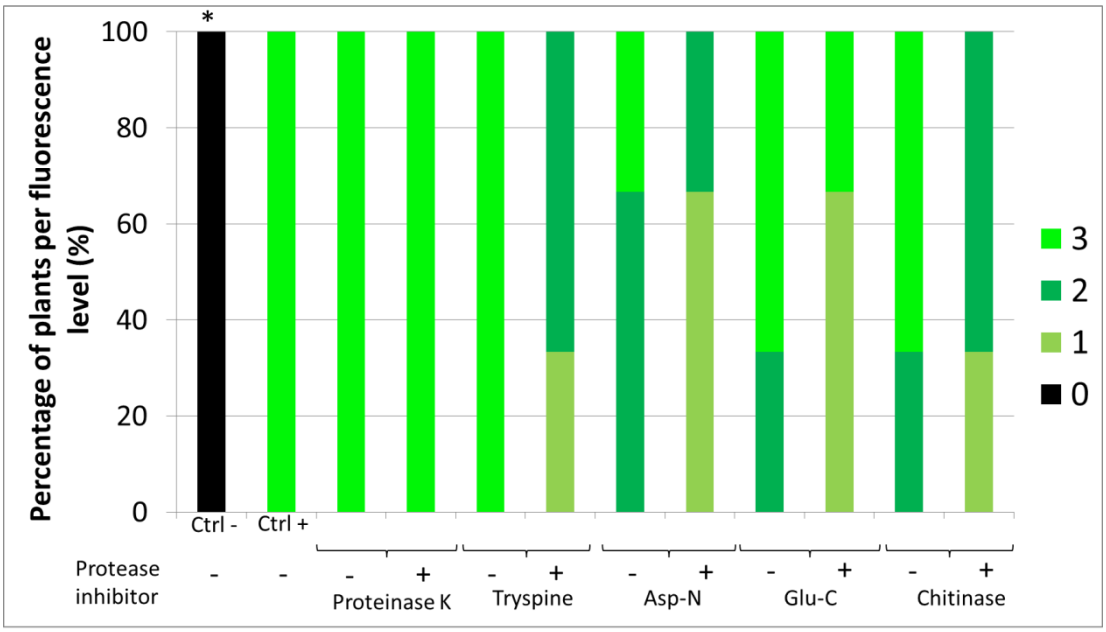

Figure 9: Effect of enzyme digestions on Pro*CgNIN* expression induction. BAP was used for negative control (Ctrl-); *F. casuarinae* supernatant was used for positive control (Ctrl+). The different enzymes were incubated with (+) or without (-) PMSF which was used as protease inhibitor at 0.3 mM. Number of plants per fluorescence level scaled 0, 1, 2, 3 was counted and converted into percentages (§2.2). Statistical significance was recorded at *p-value<0.05, n=3. Raw data are found in Appendix 3.

In our experiment, no significant differences were found between the different enzymes tested. Only the negative control (Ctrl-) was significantly different from the positive control (Ctrl+). To improve the robustness of our findings, more replicates should be performed.

No reduction of fluorescence was observed when FcS 30X was incubated with the different enzymes. **NINA is thus not sensitive to these enzymes.** However, the trend shows that fluorescence decreases when protease inhibitor (PMSF) was added, except for Proteinase K. Addition of PMSF could impact *GFP* expression. GUS results confirmed GFP fluorescence results (Appendix 3).

3.2. PRE-PURIFICATION STEPS

To identify Cg*NIN* Activator(s) (NINA), we chose to purify *F. casuarinae* supernatant containing NINA, first using NINA's hydrophobic properties, secondly using NINA's ionic charge properties and finally by combining both properties. All purification fractions obtained were tested using the plant bioassay.

3.2.1. USING HYDROPHOBIC PROPERTIES OF NINA

The SYAT team has previously tested a reverse phase C18 column (WATER Spe-Pak cartidge) to purify NINA. Even when the lowest concentration (5%) of a polar solvent such as acetonitrile was used, NINA remained unbound to the stationary phase. With a more polar solvent such as methanol, NINA was bound on the reverse phase C18 column but eluted with 10 % of methanol. **These results showed that NINA was hydrophilic with a weak hydrophobic property.**

We thus decided to test different stationary phases that were able to purify molecules based on ionic interactions.

3.2.2. USING IONIC CHARGES PROPERTIES OF NINA

We tested different ion exchange columns, W-AX (Weak Anion eXchange) and W-CX (Weak Cation eXchange) to purify NINA based on ionic charges. Elution fractions were tested using our plant bioassay (data not shown). On both W-AX and W-CX columns, NINA was bound to the stationary phases. However, fluorescence was observed in the wash step as well as in both elutions containing methanol. **These results showed that NINA was weakly charged.**

To enhance purification, we decided to test stationary phases that are able to purify molecules using both ionic interactions and hydrophobic interactions.

3.2.3. USING CHIMERIC IONIC CHARGES – HYDROPHOBIC PROPERTIES OF NINA

Following previous results, hybrid columns, Strata-X-AW and Strata-X-CW were thus used. These columns rely on two types of interactions: polar interactions and weak ion exchanges. Strata X-AW/CW columns were tested according to the protocol provided by Phenomenex (Table 1). After each step of the purification, we tested each purified fraction using our plant bioassay (Appendix 4) and results are summarized in Table 2.

Table 2: Purification of NINA using Strata-X-AW and Strata-X-CW Phenomenex columns. Negative control (BAP) showed a fluorescence median of 0 and positive control (FcS) showed a fluorescence median of 3. Number of plants per fluorescence level scaled 0, 1, 2, 3 was counted and converted into median (§2.2). Statistical significance was recorded at *p-value<0.05, n=4. Raw data are found in Appendix 4.

Steps	X-AW Fluorescence median	X-CW Fluorescence median
Load: FCS 30X + HEPES pH 7 20 mM	3	3
Flow through	0*	0*
Wash 1 – Ammonium acetate 25 mM pH 7	0*	0*
Wash 2 - Methanol 100%	1*	1*
Elution A – 5% formic acid / 95% methanol	2*	3
Elution B– 5% ammonium hydroxide / 95% methanol	3	0*

Maximum fluorescence was observed for the loading step in both columns. NINA is active before loading on both columns. No fluorescence was seen in the flow through showing that NINA binds to the stationary phases of both columns. Wash 1 (ammonium acetate 25 mM pH 7) does not elute NINA since no fluorescence was observed. However, some fluorescence was observed for wash 2 (methanol 100%), revealing thus that methanol influences NINA's interaction with both stationary phases. At elution step, fluorescence was observed for elution A (5% formic acid / 95% methanol) in both columns, while no fluorescence was recorded for X-CW elution B (5% ammonium hydroxide / 95% methanol). **We concluded that the X-CW column binds NINA more specifically than the X-AW column does.**

Since X-CW is a weak cation exchange column and that sample is loaded at pH 7, we can infer that NINA is negatively charged at input pH 7. Because of its excellent retention on the sorbent, we decided to work on X-CW for further purification. In order to continue our investigation, this procedure was optimized to improve the pre-purification of NINA.

3.2.4. OPTIMIZATION OF PRE-PURIFICATION STEPS

3.2.4.1 Loading step optimization

To optimize NINA's binding on X-CW columns, different pH conditions were tested for the loading step. Elution fractions were tested using our plant bioassay (Appendix 5) and results were summarized in Table 3.

Table 3: Effect of loading conditions on NINA binding using Strata- X-CW Phenomenex columns. Elution consists of 5 % formic acid and 95 % methanol. Negative control (BAP) showed a fluorescence median of 0 and positive control (FcS) showed a fluorescence median of 3. Number of plants per fluorescence level scaled 0, 1, 2, 3 was counted and converted into median (§2.2). Statistical significance was recorded at *p-value<0.05, n=3. Raw data are found in Appendix 5.

Loading conditions	Input fluorescence median	Fluorescence median of elution
HEPES pH 7	3	3
MES pH 7	3	2
MES pH 6	2	2
MES pH 5	3	1

In our experiment, no significant differences of fluorescence were found between the final elution steps and the control. Following MES pH 5 loading condition, fluorescence median of elution was recorded as 1 but was not significantly different from the positive control, (p-value = 0.059).

Using either HEPES or MES at pH 7, maximum fluorescence was observed in the elution step. Fluorescence for MES pH 5 loading condition was recorded as level 3. However, NINA was not well eluted. The flow through following MES pH 5 loading condition did not show any fluorescence (Appendix 5). NINA could still be bound to the column, NINA might not be stable at pH 5, as suggested by the results presented in **Figure 8**, or plants could have not responded well.

HEPES was chosen for further experiments for two reasons: HEPES buffer at pH 7 showed the best plant response (Figure 8) and it is more compatible with mass spectrometry. **Thus, the condition FcS 30X with HEPES pH 7 was selected for sample loading.**

Moreover, since the condition FcS 30X with HEPES pH 7 was selected for sample loading, to limit the pH variation, the equilibration step of the column was changed from using Ultra-Pure water at pH 7 to using HEPES buffer at pH 7.

3.2.4.2 Wash step optimization

Table 4: Effect of methanol in the wash step on the binding mechanism of NINA, using Strata-X-CW Phenomenex column. Negative control (BAP) showed a fluorescence median of 0 and positive control (FcS) showed a fluorescence median of 3. Number of plants per fluorescence level scaled 0, 1, 2, 3 was counted and converted into median (§2.2). Statistical significance was recorded at *p-value<0.05, n=8. Raw data are found in Appendix 6.

Steps	Fluorescence median
FcS 30X + HEPES pH 7	3
Flow through	0*
Ammonium acetate 25 mM pH7	0*
Methanol 10%	0*
Methanol 20%	0*
Methanol 30%	3
Methanol 50%	2.5
Methanol 100%	0*

To optimize the wash step, a gradual methanol elution was performed. Each wash was tested using the plant bioassay (Appendix 6) and results were summarized in Table 4.

Significant differences from the positive control were found for the flow through, ammonium acetate wash, methanol 10% wash, methanol 20% wash and methanol 100% wash. No significant differences from the positive control were found for the methanol 30 % and methanol 50% wash.

Fluorescence was not observed in the first wash consisting of ammonium acetate pH 7. Gradually increasing the percentage of methanol showed that NINA is eluted when 30% methanol is added. Less fluorescence is observed at 50% and 100% methanol since most of NINA has been eluted at methanol 30% (Table 4).

To optimize the purification protocol, we modified the wash step from 100% methanol to 20% methanol to maximize the elimination of non-target molecules such as high hydrophobic molecules.

3.2.4.3 Elution step choice

To elute NINA on the Strata-X-CW column, two elution conditions suggested by Phenomenex were tested (Table 2). Fluorescence was not seen for the elution containing ammonium hydroxide whereas full fluorescence was seen for the elution containing formic acid. Fluorescence observed in both elutions is significantly different. **NINA is thus eluted in a polar solvent, in acidic conditions (pH 1.8).**

Moreover, since NINA is negatively charged at pH 7 (loading condition) and eluted at pH 1.8, we can hypothesize that NINA is neutrally or positively charged at pH 1.8. Thus we can infer that $pI_{NINA} > 1.8$.

For further tests, we used an elution at pH 1.8. Moreover, an elution step was added between both washes: ammonium acetate 25 mM at pH 7 and methanol 20%. This step re-equilibrates the column in methanol to enhance the acid final elution.

3.2.4.4 NINA optimized pre-purification protocol

From all the above tests, an optimized protocol for NINA's purification (Table 5) was deduced (§2.3.3). With this protocol, NINA is eluted without losing its initial activity. It also reunites the optimized conditions for mass spectrometry analysis afterwards.

Table 5: NINA optimized pre-purification protocol on Strata- X-CW Phenomenex columns.

Steps	Solvents	Volume (mL)
Conditioning	1. Methanol 100%	10
	2. HEPES pH 7 20 mM	10
Sample loading	FcS + HEPES pH 7 20 mM	10
Wash	1. Ammonium acetate 25 mM pH 7	20
	2. Methanol 95% / Ammonium hydroxide 5% pH 11	20
	3. Methanol 20%	20
Elution	Methanol 95% / Formic Acid 5% pH 1.8	10

The conditioning step consists of first wetting the column with methanol to remove trapped air and solvates. Then, an equilibration step in HEPES pH 7 conditions the column in the same ionic strength and pH as the sample loading step. FcS 30X is loaded under pH 7 conditions to deprotonate the carboxylic groups in the stationary phase and protonate NINA. Ammonium acetate at pH 7 enhances the ionic interactions and all the water-soluble compounds that are weakly bonded are released. Then, wash 2 (ammonium hydroxide 5% / methanol 95%) at pH 11 washes out all the non-protonated molecules weakly bound to the stationary phase. Wash 3 (methanol 20%) re-equilibrates the column in methanol and enhances the acid final elution. Finally, in the elution step, the acid solution at pH 1.8 (5% formic acid / 95% methanol) ensures the protonation of the carboxylic groups of the stationary phase. This disrupts the ionic interactions with NINA.

Following the NINA optimized pre-purification protocol, we obtained a significant amount of semi-purified signal molecules to start structural analysis.

3.3. PRELIMINARY ANALYSES OF PRE-PURIFICATIONS ELUTION BY MASS SPECTROMETRY

We used the technique of mass spectrometry to elucidate the structural identity of NINA. Strata-X-CW elution fractions (Table 5) were prepared as described in (§2.3.5). These active fractions were first tested using the Quadrupole-Time Of Flight mass spectrometer, then combined with liquid chromatography.

3.3.1. Q-TOF LIQUID CHROMATOGRAPHY MASS SPECTROMETER RESULTS

Q-TOF mass spectrometry allowed us to beginning structural analysis of X-CW elution fractions. First, we injected fractions directly without a chromatographic separation (Figure 10).

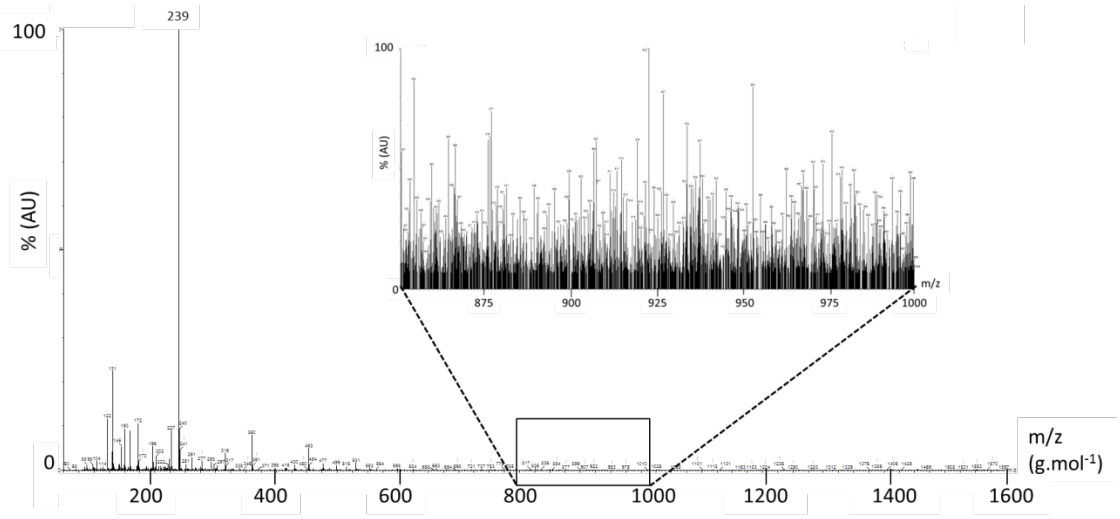

Figure 10: Mass spectra of X-CW elution fraction solubilized in Ultra-Pure water, directly injected. Zoom box of background noise between 800 and 1000 g.mol^{-1}. Detection was in Arbitrary Units (AU).

There were too many peaks and none were distinguishable from background noise. Therefore, we used Q-TOF mass spectrometry combined with high pressure liquid chromatography (LC MS/MS) to enhance the separation of the molecules and the resolution of the mass spectra. We first fractionated on a preparative C18 reverse-phase column using a water-methanol gradient as described in materials and methods and obtained the following chromatogram (Figure 11).

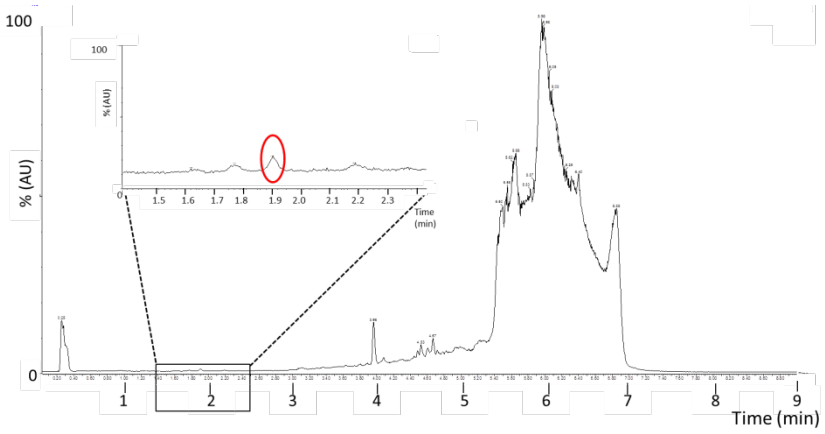

Figure 11: Chromatogram obtained using a preparative C18 reverse-phase column in LC MS/MS. Injection consisted of X-CW elution fraction (1 µL). Gradient was described in Material and Methods. Zoom box on retention time (R_T) close to void volume. Red circle indicates the fraction that will be analyze in LC MS/MS at R_T = 1.9 min. Detection was in Arbitrary Units (AU).

Previous results showed that using a reverse phase C18 column to purify NINA (§3.2.1), NINA is eluted with 10% methanol, near void volume. Thus, we will focus on the MS spectra obtained at retention time equal to 1.9 min. These fractions were compared to controls which consisted of Strata-X-CW elution fractions at pH 11 (methanol 95% / Ammonium hydroxide 5%) from (Table 5).

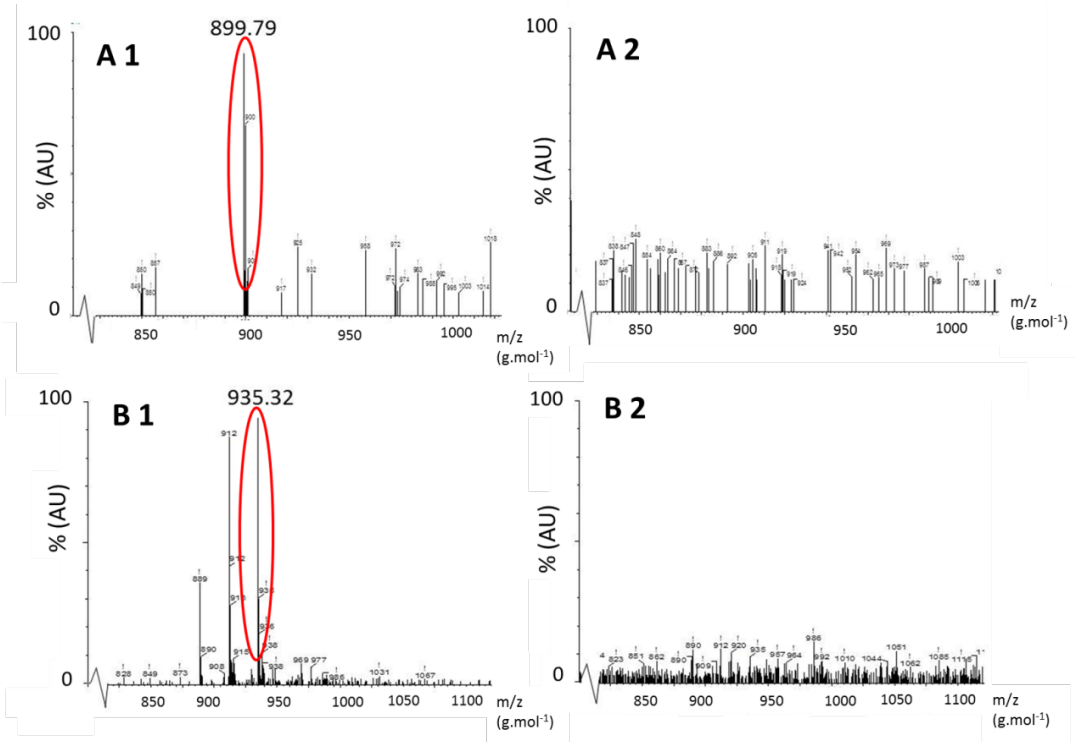

Figure 12: Mass spectra of X-CW elution fractions, first fractionated on a C_{18} reverse phase column before ionization at R_T = 1.9 min. Peaks were found in X-CW elution fractions and not in controls (red circle). **A1**: Positive ion mass spectra of X-CW elution fraction solubilized in 0.1% TFA. **A2**: positive ion mass spectra of X-CW methanol 95% / Ammonium hydroxide 5% fraction solubilized in 0.1% TFA. **B1**: Negative ion mass of X-CW elution fraction solubilized in Ultra-Pure water. **B2**: Negative ion mass spectra of X-CW methanol 95% / Ammonium hydroxide 5% fraction, solubilized in Ultra-Pure water. Detection was in Arbitrary Units (AU).

At R_T equal to 1.9 min, ionization by LCMS was performed. Molecular ion 1 ($m + H^+$ at m/z = 899.79 $g.mol^{-1}$) in the positive ion spectrum and a molecular ion 2 ($m - H^+$ at m/z = 935.32 $g.mol^{-1}$) in the negative ion spectrum were obtained (Figure 12A1; Figure 12B1). Molecular ions 1 and 2 were not found in control samples (Figure 12A2; Figure 12B2). We can infer that NINA may be either the ion molecule 1 in the positive ion spectra or the ion molecule 2 in the negative spectra. To know more about the structure of these two molecules, we used the ion trap mass spectrometer to fragment these two ion molecules.

3.3.2. ION TRAP MASS SPECTROMETER RESULTS

Using an electric field of 15 V to 45 V, the ion trap mass spectrometer was able to isolate molecule ion 2 from the negative spectra obtained in Figure 12B1. After fragmentation, we obtained molecular ion 3 ($m - 2H^+$ at m/z= 888.8 $g.mol^{-1}$) and contamination corresponding to formic acid. To know more about molecular ion 3, we applied a stronger electric field of 15 V to 60 V to isolate molecule 3. We obtained one of the possible fragmentation spectra (Figure 13).

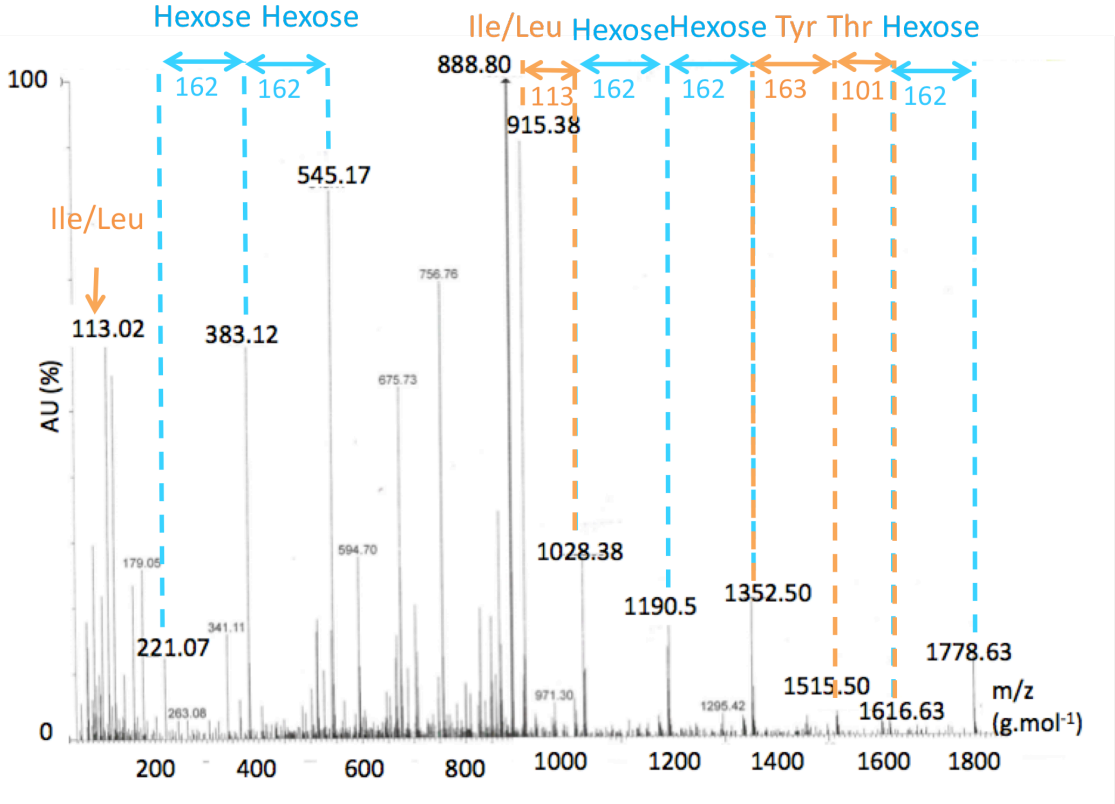

Figure 13: Ion trap spectra of molecule 3 ($M + 2H^+$ at m/z = 888.8 $g.mol^{-1}$) obtained using an electric field of 15 V to 60 V. Ion molecule 3 splits into several sugars (hexose) (blue arrows) and three amino acids (red arrows): isoleucine or leucine (Ile/Leu), tyrosine (Tyr) and threonine (Thr). Detection was in Arbitrary Units (AU).

Since a mass spectrum plots the ion signal as a function of the mass-to-charge ratio, we calculated differences of ion weights. Gaps of 162 $g.mol^{-1}$ between peaks were found which could correspond to dehydrated sugar weights. Gaps which could correspond to amino acids were also found: (101 $g.mol^{-1}$) threonine, (113 $g.mol^{-1}$) isoleucine or leucine, and (163 $g.mol^{-1}$) tyrosine. From these preliminary results, we could infer that molecular ion 3 is composed of sugars and amino acids.

Since molecular ion 3 is charged twice in the negative spectra (z = 2), we can calculate the weight of molecular ion 3 as indicated in Equation 1.

Equation 1: Weight of molecular ion 3

$$m = 888.8 \times 2 + 2 = 1779.6 \text{ g.mol}^{-1}$$

If molecular ion 3 is NINA, we can infer that NINA may have a molecular weight of 1779.6 g.mol^{-1} and composed of sugars, threonine, isoleucine or leucine and tyrosine. However, since mass spectra reveal high background noise, further purification needs to be achieved.

3.4. PURIFICATION STEP

To further purify NINA, we decided to use High Pressure Liquid Chromatography (HPLC). This method allows for a better compound separation than our pre-purification steps because of the different types of stationary phases and variety of mobile phase gradients that can be used.

We first tested a RP-C18 column, similar to the one used for Q-TOF mass spectrometer. X-CW elution fractions were injected on the RP-C18 column. Two different solvents were tested using TFA 0.1 % (v:v) or ammonium hydroxide 0.1 % (v:v) as additives. HPLC fractions of 1 mL were collected every minute and were tested using our bioassay (Appendix 7). The chromatograms obtained are shown in Figure 14A and Figure 14B.

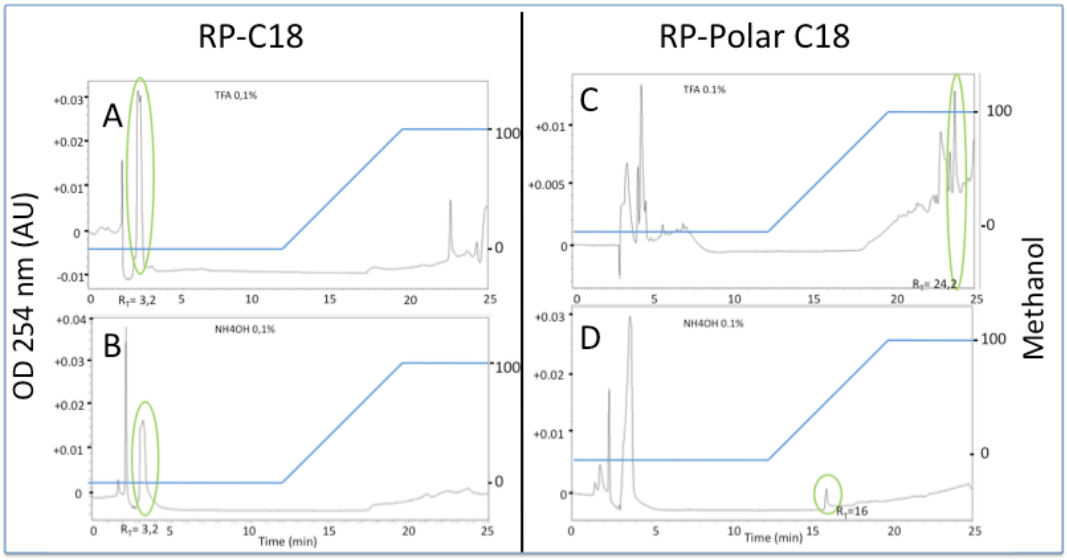

Figure 14: Chromatograms obtained using RP-C18 and RP-Polar C18 columns in HPLC. Injection consisted of X-CW elution fraction (50 µL). **A:** Purification using RP-C18 column with TFA 0.1 % (v:v). **B:** Purification using RP-C18 column with ammonium hydroxide 0.1 % (v:v). **C:** Purification using RP-Polar C18 column using TFA 0.1 % (v:v). **D:** Purification using RP-Polar C18 column using ammonium hydroxide 0.1 % (v:v). Regions circled correspond to fractions leading to the activation of Pro*CgNIN:GFP* and Pro*CgNIN:GUS*. The blue line corresponds to methanol gradient as described in Material and Methods. UV detection was at 254 nm in Arbitrary Units (AU). Raw data are found in Appendix 7 and Appendix 8.

The activity was found for a retention time (R_T) equal to 3.25 min indicating that NINA is not retained on the RP-C18 column (Figure 14A and Figure 14Figure 14B). This is similar to the results obtained with the reverse phase C18 coupled with MS. Changing additives does not impact the retention time on RP-C18 column.

X-CW elution fractions were then fractionated on a RP-Polar C18 column using the same gradient as for RP-C18. Two different additives were also tested: TFA 0.1 % (v:v) and ammonium hydroxide 0.1 % (v:v). HPLC fractions of 1 mL were collected each minute and were tested using our bioassay (Appendix 8). The chromatograms obtained are shown in Figure 14C and Figure 14D.

Under TFA conditions, activity was detected at the end of the run, R_T was equal to 24.2 min, when there is 100% methanol (Figure 14C). Resolution is low since peaks are not well separated. Under ammonium hydroxide conditions, we obtained an isolated peak, R_T was equal to 16 min, corresponding to an elution at 50% methanol (Figure 14D).

4. DISCUSSION

In this study, we purified *Frankia casuarinae* supernatant in order to elucidate the early signaling events leading to the actinorhizal nodulation process. We used a bioguided approach relying on the use of transgenic plants expressing Pro*CgNIN:GFP* or Pro*CgNIN:GUS* constructs to characterize NIN-Activator(s) (NINA). Our first aim was to develop a protocol for NINA pre-purification starting from *F. casuarinae* supernatant (FcS) and using solid phase extraction (SPE).

We first confirmed that NINA activity is not affected by pH variation, allowing us to use different pH conditions for NINA's purification. However, the trend showed that Pro*CgNIN* activation was best using HEPES buffer at pH 7 (Figure 8; Table 3) and this was mainly chosen for further experiments. The digestion of FcS by different enzymes did not yet reveal more indications on NINA's chemical nature (Figure 9). Indeed, the use of different proteinases did not modify NINA activity. However, the trend showed that fluorescence decreased when protease inhibitor (PMSF) was added. We can hypothesize that PMSF could have an inhibitor effect on NINA activity. However, more investigation is required to confirm these results. We also confirmed that NINA activity was not sensitive to the chitinase we tested from *Trichoderma viride* (Figure 9), which exhibited exo- and endochitinase activities. Our results are consistent with previous findings of Chabaud *et al.* (2016). This also confirmed the results of Cérémonie, Debellé, and Fernandez (1999) which demonstrated that *Frankia alni* Root Hair Deforming Factor was able to elicit a symbiotic response in *Alnus*, was not sensitive to chitinase. All together, these results confirmed that *Frankia* symbiotic molecule(s) signal, identified as NINA, are structurally different from rhizobial Nod factors (Chabaud *et al.*, 2016; Cissoko *et al.*, 2018).

Based on these experiments, a purification protocol using SPE was optimized and confirmed that NINA is a hydrophilic molecule (§3.2.1), which is consistent to earlier findings of Chabaud *et al.* (2016). Pre-purifications of NINA also showed that NINA is a negatively charged molecule at pH 7 (§3.2.2) and a neutrally charged molecule at pH 1.8 (§3.2.4.3). However, inferring that NINA's pI was between 1.8 and 7 is still too wide and needs to be narrowed down. Indeed, knowing NINA's charge in a certain pH environment, would guide us for further purification.

Applying our optimized purification protocol led us to obtain semi-purified active fractions that showed NINA activity. This constituted a good initial step towards the characterization of *F. casuarinae* signaling molecules.

Using mass spectrometry, we were able to identify a peak which is only present in NINA active semi-purified fraction and not in the negative control. This peak corresponds to a molecular ion that has a molecular weight of 1779.6 $g.mol^{-1}$ (Equation 1). This result is consistent with previous findings demonstrating that NINA weights between 500 Da and 3 kDa (Cissoko *et al.*, 2018). Using ion fragmentation this compound appears to be composed of sugars and amino acids, such as threonine, isoleucine and tyrosine (Figure 13).

Mass spectrometry results could explain why the enzymes did not digest NINA. We hypothesized that NINA may not have the amino acids corresponding to the cleavage

sites of the tested enzymes. Indeed, Glu-C cleaves peptide bonds on the carboxylic side and Asp-N cleaves peptide bonds on the amine side of aspartic and cysteic residues. Trypsine cleaves on the carboxyl side of lysine and arginine. However, Proteinase K cleaves peptide bonds next to the carboxyl group of aliphatic, which include isoleucine, and aromatic amino acids such as tyrosine. This contrasts with MS findings but could be explained by inaccessible cleavage sites for Proteinase K.

However, our results need to be considered with caution since MS results still show a high background noise (Figure 10). Our future work will be therefore in new ways continue and optimize NINA's purification.

Since findings revealed that NINA is a small hydrophilic molecule, the use of different HPLC columns could improve NINA purification. First results using a reverse polar stationary phase are encouraging (Figure 14) as we obtained NINA active fractions. These fractions are currently being analyzed in MS (ongoing experiment).

To enhance our pre-purification steps, a 1-butanol extraction step could be added such as the one described in Chabaud *et al.*, 2016. Since NINA is a hydrophilic molecule, the aqueous phase could be our starting material, before further purification using Strata-X-CW.

Moreover we could also improve HPLC resolution by testing a Hydrophilic Interaction Liquid Chromatography (HILIC). This technique would provide an alternative approach to effectively separate small polar compounds on polar stationary phases (Buszewski and Noga, 2012). Moreover, HILIC has many advantages and is suitable for analyzing compounds that always elute near void volume with minimal retention in reverse phase liquid chromatography (Buszewski and Noga, 2012), which was what we noticed in §3.2.1. It can also be coupled to MS and especially in the ESI mode which is the technique we used (Buszewski and Noga, 2012).

Other enzymes should be tested to continue NINA's characterization. Since MS results suggested the presence of tyrosine, pepsin enzyme could be tested as it cleaves on the carboxylic side of aromatic amino acids.

5. CONCLUSION

In this study, we investigated the nature of *F. casuarinae*'s signaling molecules in the interaction with its actinorhizal host C. glauca. Our bioassay based on the specific activation of Pro*CgNIN* by FcS helped us characterize NINA. Findings confirm that NINA is different from rhizobial Nod factors, having a potential molecular weight of 1779.6 g.mol-1, being hydrophilic, charged and resistant to the different enzymes tested, including the chitinase. Results also support the idea that NINA has a glycosylated structure and the presence of amino acids.

This study has enhanced our understanding of *Frankia* and *Casuarina* molecular dialogue, and opens to new perspectives concerning the symbiotic signalization of actinorhizal symbioses. With sufficient quantities of purified *F. casuarinae* signal molecules obtained, future work could observe the effect of purified signal molecules on *C. glauca*'s early gene expression. This way, the symbiotic signaling pathway for actinorhizal symbioses could be more detailed.

By increasing our knowledge of bacterial-plant signaling during the early stages of actinorhizal symbiosis, our study contributes to the understanding of nitrogen fixing root nodule symbioses. Indeed, plant groups that engage in root nodule symbioses all belong to the *Fabid* clade suggesting a common ancestor with a predisposition for nodulation. Exploring how legumes and actinorhizal plants have acquired this ability to fix nitrogen (Griesmann *et al.*, 2018) might provide the keys to potentially engineer the mechanisms in non-fixing crops, such as cereals, with the aim to improve food production while reducing the use of fertilizers (Good, 2018; VandenBosch and Torrey, 1985).

6. REFERENCES

Baker D. and Mullin B. 1992. Actinorhizal Symbioses. In: *Biological Nitrogen Fixation. 7*, p. 259–292.

Bargali K. 2011. Actinorhizal plants of Kumaun Himalaya and their ecological significance. *African Journal of Plant Science*. 5, p. 401–406.

Benson D.R. and Silvester W.B. 1993. Biology of Frankia strains, actinomycete symbionts of actinorhizal plants. *Microbiological Reviews*. 57(2), p. 293–319.

Berry A.M., McIntyre L., and McCully M.E. 1986. Fine structure of root hair infection leading to nodulation in the Frankia–Alnus symbiosis. *Canadian Journal of Botany*. 64(2), p. 292–305.

Buszewski B. and Noga S. 2012. Hydrophilic interaction liquid chromatography (HILIC)--a powerful separation technique. *Analytical and Bioanalytical Chemistry*. 402(1), p. 231–247.

Cérémonie H., Debellé F., and Fernandez M.P. 1999. Structural and functional comparison of Frankia root hair deforming factor and rhizobia Nod factor. *Canadian Journal of Botany*. 77(9), p. 1293–1301.

Chabaud M., Gherbi H., Pirolles E., Vaissayre V., Fournier J., Moukouanga D., Franche C., Bogusz D., Tisa L.S., Barker D.G., and Svistoonoff S. 2016. Chitinase-resistant hydrophilic symbiotic factors secreted by Frankia activate both Ca2+ spiking and NIN gene expression in the actinorhizal plant Casuarina glauca. *New Phytologist*. 209(1), p. 86–93.

Chaia E., Wall L.G., and Huss-Danell K. 2010. Life in soil by the actinorhizal root nodule endophyte Frankia. *Symbiosis*. 51(3), p. 201–226.

Cissoko M., Hocher V., Gherbi H., Gully D., Carre-Mlouka A., Sane S., Pignoly S., Champion A., Ngom M., Pujic P., Fournier P., Gtari M., Swanson E., Pesce C., Tisa L.S., Sy M., and Svistoonoff S. 2018. Actinorhizal signaling molecules: Frankia root hair deforming factor shares properties with NIN induction factor. *Manuscript submitted for publication in Frontiers in Plant Science*.

Clavijo F., Diedhiou I., Vaissayre V., Brottier L., Acolatse J., Moukouanga D., Crabos A., Auguy F., Franche C., Gherbi H., Champion A., Hocher V., Barker D., Bogusz D., Tisa L.S., and Svistoonoff S. 2015. The Casuarina NIN gene is transcriptionally activated throughout Frankia root infection as well as in response to bacterial diffusible signals. *The New Phytologist*. 208(3), p. 887–903.

Dawson J.O. 2008. Ecology Of Actinorhizal Plants. In : Pawlowski K., Newton W.E. (eds.). *Nitrogen-fixing Actinorhizal Symbioses*. Dordrecht : Springer Netherlands, p. 199–234.

Demina I.V., Persson T., Santos P., Plaszczyca M., and Pawlowski K. 2013. Comparison of the nodule vs. root transcriptome of the actinorhizal plant Datisca glomerata: actinorhizal nodules contain a specific class of defensins. *PloS One*. 8(8), p. e72442.

Dénarié J., Debellé F., and Promé J.C. 1996. Rhizobium lipo-chitooligosaccharide nodulation factors: signaling molecules mediating recognition and morphogenesis. *Annual Review of Biochemistry*. 65, p. 503–535.

Diagne N., Arumugam K., Ngom M., Nambiar-Veetil M., Franche C., Narayanan K.K., and Laplaze L. 2013. Use of Frankia and actinorhizal plants for degraded lands reclamation. *BioMed Research International*. 2013, p. 948258.

Gherbi H., Markmann K., Svistoonoff S., Estevan J., Autran D., Giczey G., Auguy F., Péret B., Laplaze L., Franche C., Parniske M., and Bogusz D. 2008. SymRK defines a common genetic basis for plant root endosymbioses with arbuscular mycorrhiza fungi, rhizobia, and Frankiabacteria. *Proceedings of the National Academy of Sciences*. 105(12), p. 4928–4932.

Good A. 2018. Toward nitrogen-fixing plants. *Science*. 359(6378), p. 869–870.

Granqvist E., Sun J., Op den Camp R., Pujic P., Hill L., Normand P., Morris R.J., Downie J.A., Geurts R., and Oldroyd G.E.D. 2015. Bacterial-induced calcium oscillations are common to nitrogen-fixing associations of nodulating legumes and nonlegumes. *The New Phytologist*. 207(3), p. 551–558.

Griesmann M., Chang Y., Liu X., Song Y., Haberer G., Crook M.B., Billault-Penneteau B., Lauressergues D., Keller J., Imanishi L., Roswanjaya Y.P., Kohlen W., Pujic P., Battenberg K., Alloisio N., Liang Y., Hilhorst H., Salgado M.G., Hocher V., Gherbi H., Svistoonoff S., Doyle J.J., He S., Xu Y., Xu S., Qu J., Gao Q., Fang X., Fu Y., Normand P., Berry A.M., Wall L.G., Ané J.-M., Pawlowski K., Xu X., Yang H., Spannagl M., Mayer K.F.X., Wong G.K.-S., Parniske M., Delaux P.-M., and Cheng S. 2018. Phylogenomics reveals multiple losses of nitrogen-fixing root nodule symbiosis. *Science*. 361(6398), p. 1743.

Guillotin B., Couzigou J.-M., and Combier J.-P. 2016. NIN Is Involved in the Regulation of Arbuscular Mycorrhizal Symbiosis. *Frontiers in Plant Science*. 7.

Hocher V., Alloisio N., Auguy F., Fournier P., Doumas P., Pujic P., Gherbi H., Queiroux C., Silva C.D., Wincker P., Normand P., and Bogusz D. 2011. Transcriptomics of Actinorhizal Symbioses Reveals Homologs of the Whole Common Symbiotic Signaling Cascade. *Plant Physiology*. 156(2), p. 700–711.

Hocher V., Auguy F., Argout X., Laplaze L., Franche C., and Bogusz D. 2006. Expressed sequence-tag analysis in Casuarina glauca actinorhizal nodule and root. *New Phytologist*. 169(4), p. 681–688.

Hoffman B.M., Lukoyanov D., Yang Z.-Y., Dean D.R., and Seefeldt L.C. 2014. Mechanism of nitrogen fixation by nitrogenase: the next stage. *Chemical Reviews*. 114(8), p. 4041–4062.

Ktari A., Gueddou A., Nouioui I., Miotello G., Sarkar I., Ghodhbane-Gtari F., Sen A., Armengaud J., and Gtari M. 2017. Host Plant Compatibility Shapes the Proteogenome of Frankia coriariae. *Frontiers in Microbiology*. 8, p. 720.

Kucho K.-I., Kakoi K., Yamaura M., Higashi S., Uchiumi T., and Abe M. 2009. Transient transformation of frankia by fusion marker genes in liquid culture. *Microbes and Environments*. 24(3), p. 231–240.

Lerouge P., Roche P., Faucher C., Maillet F., Truchet G., Promé J.C., and Dénarié J. 1990. Symbiotic host-specificity of Rhizobium meliloti is determined by a sulphated and acylated glucosamine oligosaccharide signal. *Nature*. 344(6268), p. 781–784.

Markmann K., Giczey G., and Parniske M. 2008. Functional Adaptation of a Plant Receptor- Kinase Paved the Way for the Evolution of Intracellular Root Symbioses with Bacteria. *PLOS Biology*. 6(3), p. e68.

Miller I.M. and Baker D.D. 1986. Nodulation of actinorhizal plants byFrankia strains capable of both root hair infection and intercellular penetration. *Protoplasma*. 131(1), p. 82–91.

Nguyen T.V., Wibberg D., Battenberg K., Blom J., Vanden Heuvel B., Berry A.M., Kalinowski J., and Pawlowski K. 2016. An assemblage of Frankia Cluster II strains from California contains the canonical nod genes and also the sulfotransferase gene nodH. *BMC Genomics*. 17(1), p. 796.

Normand P., Lapierre P., Tisa L.S., Gogarten J.P., Alloisio N., Bagnarol E., Bassi C.A., Berry A.M., Bickhart D.M., Choisne N., Couloux A., Cournoyer B., Cruveiller S., Daubin V., Demange N., Francino M.P., Goltsman E., Huang Y., Kopp O.R., Labarre L., Lapidus A., Lavire C., Marechal J., Martinez M., Mastronunzio J.E., Mullin B.C., Niemann J., Pujic P., Rawnsley T., Rouy Z., Schenowitz C., Sellstedt A., Tavares F., Tomkins J.P., Vallenet D., Valverde C., Wall L.G., Wang Y., Medigue C., and Benson D.R. 2007. Genome characteristics of facultatively symbiotic Frankia sp. strains reflect host range and host plant biogeography. *Genome Research*. 17(1), p. 7–15.

Normand P., Orso S., Cournoyer B., Jeannin P., Chapelon C., Dawson J., Evtushenko L., and Misra A.K. 1996. Molecular phylogeny of the genus Frankia and related genera and emendation of the family Frankiaceae. *International Journal of Systematic Bacteriology*. 46(1), p. 1–9.

Nouioui I., Ghodhbane-Gtari F., Montero-Calasanz M.D.C., Göker M., Meier-Kolthoff J.P., Schumann P., Rohde M., Goodfellow M., Fernandez M.P., Normand P., Tisa L.S., Klenk H.-P., and Gtari M. 2016. Proposal of a type strain for Frankia alni (Woronin 1866) Von Tubeuf 1895, emended description of Frankia alni, and recognition of Frankia casuarinae sp. nov. and Frankia elaeagni sp. nov. *International Journal of Systematic and Evolutionary Microbiology*. 66(12), p. 5201–5210.

Obertello M., Mame O.S., Laurent L., Carole S., Sergio S., Florence A., Didier B., and Claudine F. 2003. Actinorhizal nitrogen fixing nodules: infection process,

molecular biology and genomics. *African Journal of Biotechnology*. 2(12), p. 528–538.

Oldroyd G.E.D. 2013. Speak, friend, and enter: signalling systems that promote beneficial symbiotic associations in plants. *Nature Reviews. Microbiology*. 11(4), p. 252–263.

Oldroyd G.E.D., Murray J.D., Poole P.S., and Downie J.A. 2011. The rules of engagement in the legume-rhizobial symbiosis. *Annual Review of Genetics*. 45, p. 119–144.

Olivares J., Bedmar E.J., and Sanjuán J. 2013. Biological nitrogen fixation in the context of global change. *Molecular plant-microbe interactions: MPMI*. 26(5), p. 486–494.

Pawlowski K. and Demchenko K.N. 2012. The diversity of actinorhizal symbiosis. *Protoplasma*. 249(4), p. 967–979.

Péret B., Swarup R., Jansen L., Devos G., Auguy F., Collin M., Santi C., Hocher V., Franche C., Bogusz D., Bennett M., and Laplaze L. 2007. Auxin Influx Activity Is Associated with Frankia Infection during Actinorhizal Nodule Formation in Casuarina glauca. *Plant Physiology*. 144(4), p. 1852–1862.

Perrine-Walker F., Gherbi H., Imanishi L., Hocher V., Ghodhbane-Gtari F., Lavenus J., Benabdoun F.M., Nambiar-Veeti M., Svistoonoff S., and Laplaze L. 2011. Symbiotic signaling in actinorhizal symbioses. *Current Protein & Peptide Science*. 12(2), p. 156–164.

Persson T., Battenberg K., Demina I.V., Vigil-Stenman T., Heuvel B.V., Pujic P., Facciotti M.T., Wilbanks E.G., O'Brien A., Fournier P., Hernandez M.A.C., Herrera A.M., Médigue C., Normand P., Pawlowski K., and Berry A.M. 2015. Candidatus Frankia Datiscae Dg1, the Actinobacterial Microsymbiont of Datisca glomerata, Expresses the Canonical nod Genes nodABC in Symbiosis with Its Host Plant. *PLOS ONE*. 10(5), p. e0127630.

Phenomenex. 2017. *The Complete Guide to Solid Phase Extraction (SPE) | Phenomenex UHPLC, HPLC, SPE and GC*. Phenomenex

Postgate J.R. 1982. Biological nitrogen fixation: fundamentals. *Phil. Trans. R. Soc. Lond. B*. 296(1082), p. 375–385.

Rawnsley T. and Tisa L.S. 2007. Development of a physical map for three Frankia strains and a partial genetic map for Frankia EuI1c. Available at : < http://www.ingentaconnect.com/content/mksg/ppl/2007/00000130/00000003/art00013 > (Accessed : 25 August 2018).

Rouvier C., Schwencke J., Prin Y., Navarro E., Benoist P., Müller A., Girgis M., Selim S., Reddell P., Gauthier D., Rinaudo G., Normand P., and Simonet P. 1996. Biologie et diversité génétique des souches de *Frankia* associées aux Casuarinacées. *Acta Botanica Gallica*. 143(7), p. 567–580.

Santi C., Bogusz D., and Franche C. 2013. Biological nitrogen fixation in non-legume plants. *Annals of Botany*. 111(5), p. 743–767.

Simonet P., Navarro E., Rouvier C., Reddell P., Zimpfer J., Dommergues Y., Bardin R., Combarro P., Hamelin J., Domenach A.-M., Gourbière F., Prin Y., Dawson J.O., and Normand P. 1999. Co-evolution between Frankia populations and host plants in the family Casuarinaceae and consequent patterns of global dispersal. *Environmental Microbiology*. 1(6), p. 525–533.

Soltis D.E., Soltis P.S., Morgan D.R., Swensen S.M., Mullin B.C., Dowd J.M., and Martin P.G. 1995. Chloroplast gene sequence data suggest a single origin of the predisposition for symbiotic nitrogen fixation in angiosperms. *Proceedings of the National Academy of Sciences*. 92(7), p. 2647–2651.

Soyano T., Kouchi H., Hirota A., and Hayashi M. 2014. Nodule inception directly targets NF-Y subunit genes to regulate essential processes of root nodule development in Lotus japonicus. *PLoS genetics*. 9(3), p. e1003352.

Svistoonoff S., Benabdoun F.M., Nambiar-Veetil M., Imanishi L., Vaissayre V., Cesari S., Diagne N., Hocher V., de Billy F., Bonneau J., Wall L., Ykhlef N., Rosenberg C., Bogusz D., Franche C., and Gherbi H. 2013. The Independent Acquisition of Plant Root Nitrogen-Fixing Symbiosis in Fabids Recruited the Same Genetic Pathway for Nodule Organogenesis. *PloS one*. 8(5), p. e64515.

Svistoonoff S., Gherbi H., Nambiar-Veetil M., Zhong C., Michalak Z., Laplaze L., Vaissayre V., Auguy F., Hocher V., Doumas P., Bonneau J., Bogusz D., and Franche C. 2010. Contribution of transgenic Casuarinaceae to our knowledge of the actinorhizal symbioses. *Symbiosis*. 50(1), p. 3–11.

Svistoonoff S., Hocher V., and Gherbi H. 2014. Actinorhizal root nodule symbioses: what is signalling telling on the origins of nodulation? *Current Opinion in Plant Biology*. 20, p. 11–18.

Tisa L.S., Oshone R., Sarkar I., Ktari A., Sen A., and Gtari M. 2016. Genomic approaches toward understanding the actinorhizal symbiosis: an update on the status of the Frankia genomes. *Symbiosis*. 70(1), p. 5–16.

Valdés M., Pérez N.-O., Estrada-de los Santos P., Caballero-Mellado J., Peña-Cabriales J.J., Normand P., and Hirsch A.M. 2005. Non-Frankia Actinomycetes Isolated from Surface-Sterilized Roots of Casuarina equisetifolia Fix Nitrogen. *Applied and Environmental Microbiology*. 71(1), p. 460–466.

VandenBosch K.A. and Torrey J.G. 1985. Development of Endophytic Frankia Sporangia in Field- and Laboratory-Grown Nodules of Comptonia peregrina and Myrica Gale. *American Journal of Botany*. 72(1), p. 99–108.

Vessey J., Pawlowski K., and Bergman B. 2005. Root-based N2-fixing Symbioses: Legumes, Actinorhizal Plants, Parasponia sp. and Cycads. In : *Plant and Soil*. p. 51–78.

Yoro E., Suzaki T., Toyokura K., Miyazawa H., Fukaki H., and Kawaguchi M. 2014. A Positive Regulator of Nodule Organogenesis, NODULE INCEPTION, Acts as a Negative Regulator of Rhizobial Infection in Lotus japonicus1[W]. *Plant Physiology*. 165(2), p. 747–758.

Zhang X. and Benson D.R. 1992. Utilization of amino acids by Frankia sp. strain CpI1. *Archives of Microbiology*. 158(4), p. 256–261.

Zhang Z., Lopez M.F., and Torrey J.G. 1984. A comparison of cultural characteristics and infectivity of Frankia isolates from root nodules of Casuarina species. *Plant and Soil*. 78(1/2), p. 79–90.

Zhong C., Mansour S., Nambiar-Veetil M., Bogusz D., and Franche C. 2013. Casuarina glauca: a model tree for basic research in actinorhizal symbiosis. *Journal of Biosciences*. 38(4), p. 815–823.

Zhong C., Zhang Y., Chen Y., Jiang Q., Chen Z., Liang J., Pinyopusarerk K., Franche C., and Bogusz D. 2009. Casuarina research and applications in China. *Symbiosis*. 50, p. 107–114.

7. LIST OF ABBREVIATIONS

AM: Arbuscular mycorrhiza

AU: Arbitrary Units

BD: Broughton and Dilworth

CCaMK: Calcium & Calmodulin-dependent Kinase

CcI3: *Frankia* strain

*Cg*NIN: *Casuarina glauca NIN*

ESI: Electrospray ionization

EST: Expressed Sequence Tag

FcS: *Frankia casuarinae* supernatant

GFP: Green Fluorescent Protein

GUS: β-glucuronidase enzyme

HPLC: High Pressure Liquid Chromatography

IPCC: Intergovernmental Panel on Climate Change

IRD: Research Institute for Development

LC/MS: Liquid chromatography paired with mass spectrometry

lj*NIN*: *Lotus japonicus NIN*

MS: Mass Spectrometry

NF: Nod factors

NIN: Nodule inception

NINA: NIN - Activator

pI: Isoelectric point

PMSF: Phenylmethylsulfonyl fluoride

Q-TOF: Quadruple Time Of Flight

RHDF: Root Hair Deforming Factor

SYMRK: SYMbiosis Receptor Kinase

T-DNA: Transfer Deoxyribonucleic acid

TFA: Trifluoroacetic acid

USDA: United States Department of Agriculture

X-Gluc: 5-bromo-4-chloro-3-indolyl glucuronide

8. TABLE OF TABLES

9. TABLE OF FIGURES